Spontaneous Room Temperature Elongation of CdS and Ag$_2$S Nanorods via Oriented Attachment

Catriona O'Sullivan,[†] Robert D. Gunning,[†,‡] Ambarish Sanyal,[†]
Christopher A. Barrett,[†] Hugh Geaney,[†] Fathima R. Laffir,[†] Shafaat Ahmed,[†] and
Kevin M. Ryan*,[†,‡]

*Materials and Surface Science Institute, Department of Chemical and Environmental Sciences, and
SFI- Strategic Research Cluster in Solar Energy Research, University of Limerick, Limerick, Ireland*

Received April 9, 2009; E-mail: kevin.m.ryan@ul.ie

Abstract: Spontaneous elongation from nanorod to nanowire in the presence of an amine is reported for nanocrystals of cadmium sulfide and silver sulfide (cation exchanged from CdS). Elongation occurs instantaneously where the final aspect ratio is a controllable multiple of the original nanorod length. Transmission electron microscopy (TEM) analysis reveals the influential factors on the attachment process are the concentration of amine, duration and temperature of the reaction. The elongated nanorods are further characterized by X-ray diffraction (XRD), photoluminescence (PL), ultraviolet−visible spectroscopy (UV−vis) and X-ray photoelectron spectroscopy (XPS). A mechanism of oriented attachment is evidenced by the doubling in length of asymmetrically gold tipped CdS nanorods with the corresponding absence of elongation in symmetrically tipped nanorods.

1. Introduction

The discovery that selective surfactant passivation can tune growth in colloidal nanocrystals along a specific growth direction to form nanorods has led to several shape-specific applications. Compared to pseudospherical nanocrystals, nanorods exhibit higher photon absorption cross sections, optical gain lifetimes, stronger electric dipoles, and linearly polarized emission of light.[1−7] These properties have resulted in nanorod integration in particular as LEDs,[8,9] single electron devices,[10,11] and type II solar-cells.[12] In a typical II−VI colloidal nanorod synthesis, for example, CdS, after initial nucleation through injection of monomer, preferred growth along the (001) direction occurs in the presence of selected surfactants which passivate competing growth facets. Typically growth occurs atom by atom at approximately 1 nm per minute until all the monomer is used. The separation of the nucleation and growth phases allows a high yield of nanorods with monodispersity in both length and diameter.[13] In a single injection, aspect ratios (L/D) of up to 6 are achievable, with additional dropwise monomer injection typically needed to achieve longer nanorods or nanowires. A disadvantage to sequential injection is, in addition to further (001) growth on each rod, the additional injections result in further nuclei with a resultant increase in polydispersity.[14] Also, the ratio of stacking faults in the elongated nanowires is significantly larger than in a single injection synthesis.[15,16] The crystal structure of the initial "seed nanocrystal" determines whether a single growth direction or several (branched growth) occurs.

Oriented attachment is an attractive route for the formation of high aspect ratio nanowires occurring from the sequential amalgamation of existing nanocrystals in solution along a preferred facet. The attachment is thermodynamically favored on the facet containing the largest number of dangling bonds which leads to the removal of surface energy which is kinetically favored at the nanoscale.[17] The formation of nanowires (aspect ratio >10) and nanorods (aspect ratio <10) from oriented attachment of pseudospherical nanocrystals has been observed in a wide range of semiconductor nanocrystals including

[†] Materials and Surface Science Institute and Department of Chemical and Environmental Sciences.
[‡] SFI- Strategic Research Cluster in Solar Energy Research.

(1) Hu, J.; Li, L.-S.; Yang, W.; Manna, L.; Wang, L.-W.; Alivisatos, A. P. *Science* **2001**, *292*, 2060−2063.
(2) Kan, S.; Mokari, T.; Rothenberg, E.; Banin, U. *Nat. Mater.* **2003**, *2*, 155−158.
(3) Buhro, W. E.; Colvin, V. L. *Nat. Mater.* **2003**, *2*, 138−139.
(4) Nann, T.; Schneider, J. *Chem. Phys. Lett.* **2004**, *384*, 150−152.
(5) Saunders, A. E.; Ghezelbash, A.; Sood, P.; Korgel, B. A. *Langmuir* **2008**, *24*, 9043−9049.
(6) Li, L.-S.; Alivisatos, A. P. *Phy. Rev. Lett.* **2003**, *90*, 097402.
(7) Ghezelbash, A.; Koo, B.; Korgel, B. A. *Nano Lett.* **2006**, *6*, 1832−1836.
(8) Nizamoglu, S.; Mutlugun, E.; Akyuz, O.; Perkgoz, N. K.; Demir, H. V.; Liebscher, L.; Sapra, S.; Gaponik, N.; Eychmuller, A. *20th Annual Meeting of the IEEE-Lasers-and-Electro-Optics-Society*; Ieee: Lake Buena Vista, FL, 2007; pp 602−603.
(9) Coe, S.; Woo, W.-K.; Bawendi, M.; Bulovic, V. *Nature* **2002**, *420*, 800−803.
(10) Klein, D. L.; Roth, R.; Lim, A. K. L.; Alivisatos, A. P.; McEuen, P. L. *Nature* **1997**, *389*, 699−701.
(11) Thelander, C.; Martensson, T.; Bjork, M. T.; Ohlsson, B. J.; Larsson, M. W.; Wallenberg, L. R.; Samuelson, L. *Appl. Phys. Lett.* **2003**, *83*, 2052−2054.
(12) Huynh, W. U.; Dittmer, J. J.; Alivisatos, A. P. *Science* **2002**, *295*, 2425−2427.

(13) Peng, X.; Manna, L.; Yang, W.; Wickham, J.; Scher, E.; Kadavanich, A.; Alivisatos, A. P. *Nature* **2000**, *404*, 59−61.
(14) Shieh, F.; Saunders, A. E.; Korgel, B. A. *J. Phys. Chem. B* **2005**, *109*, 8538−8542.
(15) Kang, C.-C.; Lai, C.-W.; Peng, H.-C.; Shyue, J.-J.; Chou, P.-T. *Small* **2007**, *3*, 1882−1885.
(16) Manna, L.; Scher, E. C.; Alivisatos, A. P. *J. Am. Chem. Soc.* **2000**, *122*, 12700−12706.
(17) Penn, R. L.; Banfield, J. F. *Geo. Et Cos. Acta* **1999**, *63*, 1549−1557.

II−VI,[18−22] V−VI,[23,24] IV−VI,[25−27] and I−VI[28] systems. In general, the attaching nanoparticles must be ligand free on the joining facet, for attachment to occur and several reports demonstrate oriented attachment only after selective removal of surfactant capping ligands.[29−31] Two distinct types of oriented attachment are reported, perfect and imperfect, depending on whether the area at which the nanocrystals fuse is apparent in the resulting nanorod.[22,32,33] The type of attachment is largely determined by the extent of Ostwald ripening which occurs in solution allowing the formation of a crystallographically smooth interface. Although oriented attachment occurs nanocrystal by nanocrystal, it is difficult to control the final aspect ratio, with a significant polydispersity in the resultant nanowires observed in approaches reported to date.

In contrast to 0D−0D nanocrystal oriented attachment,[34,35] 1D−1D attachment has not been significantly observed most likely due to the steric barrier to orientation in solution. Here we report a post synthetic, solution based process that leads to the instantaneous oriented attachment of both CdS and Ag₂S (cation exchanged from CdS) nanorods into monodispersed nanowires. The reaction is initiated by the addition of an amine which selectively depassivates the (001) facets allowing end to end fusion. Through a series of amine washing steps the nanorod length can be elongated to either double, triple or quadruple the original nanorod length with excellent control. In experiments where either one or both ends of the CdS nanorods were tipped with gold prior to elongation, doubling of the rod length occurred in asymmetrically tipped rods with no elongation in their symmetrically tipped analogues. This facile approach to nanorod elongation will likely find significant application where high aspect ratio nanorods are needed in both high yields and monodispersity.

2. Experimental Section

Additional experimental details can be found in Supporting Information.

(18) Xiong, Y.; Zhang, J.; Huang, F.; Ren, G.; Liu, W.; Li, D.; Wang, C.; Lin, Z. *J. Phy. Chem. C* **2008**, *112*, 9229−9233.
(19) Pradhan, N.; Xu, H.; Peng, X. *Nano Lett.* **2006**, *6*, 720−724.
(20) Cao, X.; Lan, X.; Guo, Y.; Zhao, C. *Cryst. Growth Des.* **2008**, *8*, 575−580.
(21) Yong, K.-T.; Sahoo, Y.; Zeng, H.; Swihart, M. T.; Minter, J. R.; Prasad, P. N. *Chem. Mater.* **2007**, *19*, 4108−4110.
(22) Claudia Pacholski, A. K. H. W. *Angew. Chem.* **2002**, *41*, 1188−1191.
(23) Deng, Y.; Nan, C.-W.; Guo, L. *Chem. Phys. Lett.* **2004**, *383*, 572−576.
(24) Lu, Q.; Zeng, H.; Wang, Z.; Cao, X.; Zhang, L. *Nanotechnology* **2006**, *17*, 2098−2104.
(25) Hawaldar, R. R.; Sathaye, S. D.; Harle, A.; Gholap, R. S.; Patil, K. R. *J. Phys. Chem. C* **2008**, *112*, 7557−7561.
(26) Zhang, J.; Wang, Y.; Zheng, J.; Huang, F.; Chen, D.; Lan, Y.; Ren, G.; Lin, Z.; Wang, C. *J. Phys. Chem. B* **2007**, *111*, 1449−1454.
(27) Cho, K.-S.; Talapin, D. V.; Gaschler, W.; Murray, C. B. *J. Am. Chem. Soc.* **2005**, *127*, 7140−7147.
(28) Yang, L.; Yang, H.; Yang, Z.; Cao, Y.; Ma, X.; Lu, Z.; Zheng, Z. *J. Phys. Chem. B* **2008**, *112*, 9795−9801.
(29) Riehle, F. S.; Bienert, R.; Thomann, R.; Urban, G. A.; Krulìger, M. *Nano Lett.* **2009**, *9*, 514−518.
(30) Tang, Z.; Kotov, N. A.; Giersig, M. *Science* **2002**, *297*, 237−240.
(31) Rakovich, Y. P.; Volkov, Y.; Sapra, S.; Susha, A. S.; Doblinger, M.; Donegan, J. F.; Rogach, A. L. *J. Phys. Chem. C* **2007**, *111*, 18927−18931.
(32) Du, N.; Zhang, H.; Chen, B.; Ma, X.; Yang, D. *J. Phys. Chem. C* **2007**, *111*, 12677−12680.
(33) Fang, Z.; Tang, K.; Gao, L.; Lei, S.; Sheng, J.; Liang, Z. *Mater. Lett.* **2006**, *60*, 1347−1349.
(34) Huang, F.; Zhang, H.; Banfield, J. F. *Nano Lett.* **2003**, *3*, 373−378.
(35) Zhang, J.; Lin, Z.; Lan, Y.; Ren, G.; Chen, D.; Huang, F.; Hong, M. *J. Am. Chem. Soc.* **2006**, *128*, 12981−12987.

2.1. Washing Step to Elongate the Nanorods. In a typical reaction, 0.018 mol amine was injected into 15 mL of nanorod solution (1.77⁻⁵ M) and the resulting mixture was sonicated for 30 s before being precipitated with acetone. The solution was then centrifuged at 3000 rpm for 3 min. The supernatant (colorless) was decanted off and the above process repeated for additional elongation steps. For time and temperature dependent reactions there was no centrifugation or sonication step, showing that agitation was not necessary for this elongation process to work.

2.2. Gold Tip Growth. Gold tip growth on the nanorods was performed according to previously reported methods.[36] The gold solution consisted of 22.5 mg of Dodecylamine (DDA), 12.5 mg of didodecyldimethylammoniumbromide (DDAB), 4 mg of AuCl in 2 mL of anhydrous toluene. The solution was prepared under nitrogen and was sonicated for 5 min before use. The cadmium sulfide nanorods solvated in toluene was placed in a three neck flask under a flow of argon. The gold solution was injected swiftly into a vigorously stirred mixture. The reaction was allowed to proceed for 2−30 min (depending on whether asymmetric or symmetric gold growth was required) before being quenched with methanol.

2.3. Characterization. Powder X-ray diffraction (XRD) spectra were obtained using silicon disks with a Philips X'Pert PRO MPD (Multipurpose X-ray Diffractometer) using Cu Kα radiation. Due to the small volume of sample available it was drop cast directly on the glass slide. Transmission electron microscopy (TEM) was performed using JEOL 2011 TEM with an accelerating voltage of 200 kV. The nanorods solvated in toluene were drop cast directly onto a carbon coated copper TEM grid and allowed to dry. X-ray Photoelectron Spectroscopy (XPS) were obtained by a Kratos Axis 165 spectrometer using monochromatic Al Kα radiation ($\lambda\nu$ = 1486.58 eV) and fixed analyzer pass energy of 20 eV. All spectra were calibrated using the C 1S at 284.8 eV.

3. Results and Discussion

Figure 1a shows a TEM image of CdS nanorods, synthesized by the colloidal route which yielded a mean length of 34 nm as shown by the size distribution curve (Figure 1g), measured from several TEM images. This nanorod solution in toluene (15 mL of 1.77⁻⁵ M), was subjected to amine (0.018 mol) wash for 30 and 120 s. The nanorods showed noticeable elongation after 30s, with random doubling and tripling of a significant percentage of the nanorods (Figure 1b). After 120 s exposure, further elongation is observed where the majority of rods at 100 and 130 nm respectively are now triple or quadruple the starting rod length (Figure 1c). The rate of elongation is also dependent on amine concentration and this was verified when the amine concentration was increased (0.030 mol) and the above experiment was repeated. After 30 s, the nanorods have mainly tripled and quadrupled in length (Figure 1d). The introduction of agitation through sonication was also effective in further reducing the reaction time for elongation. For example at lower concentrations of amine (0.018 mol), after 30 s (Figure 1e), a uniform bimodal distribution centered around 66 and 101 nm (Figure 1h) corresponds to doubling and tripling of the nanorod length. An additional injection of amine and agitation for another 30 s allows a highly uniform rod length of 131 nm to be obtained with excellent monodispersity in the resultant sample (Figure 1f), clearly shown in the size distribution curve (Figure 1i). Addition of agitation to the reaction reduces the polydispersity in rod length by creating more fusion events. The elongated rods are epitaxial in the wurtzite crystal structure and show perfect oriented attachment with no visual evidence of the

(36) O'Sullivan, C.; Ahmed, S.; Ryan, K. M. *J. Mater. Chem.* **2008**, *18*, 5218−5222.
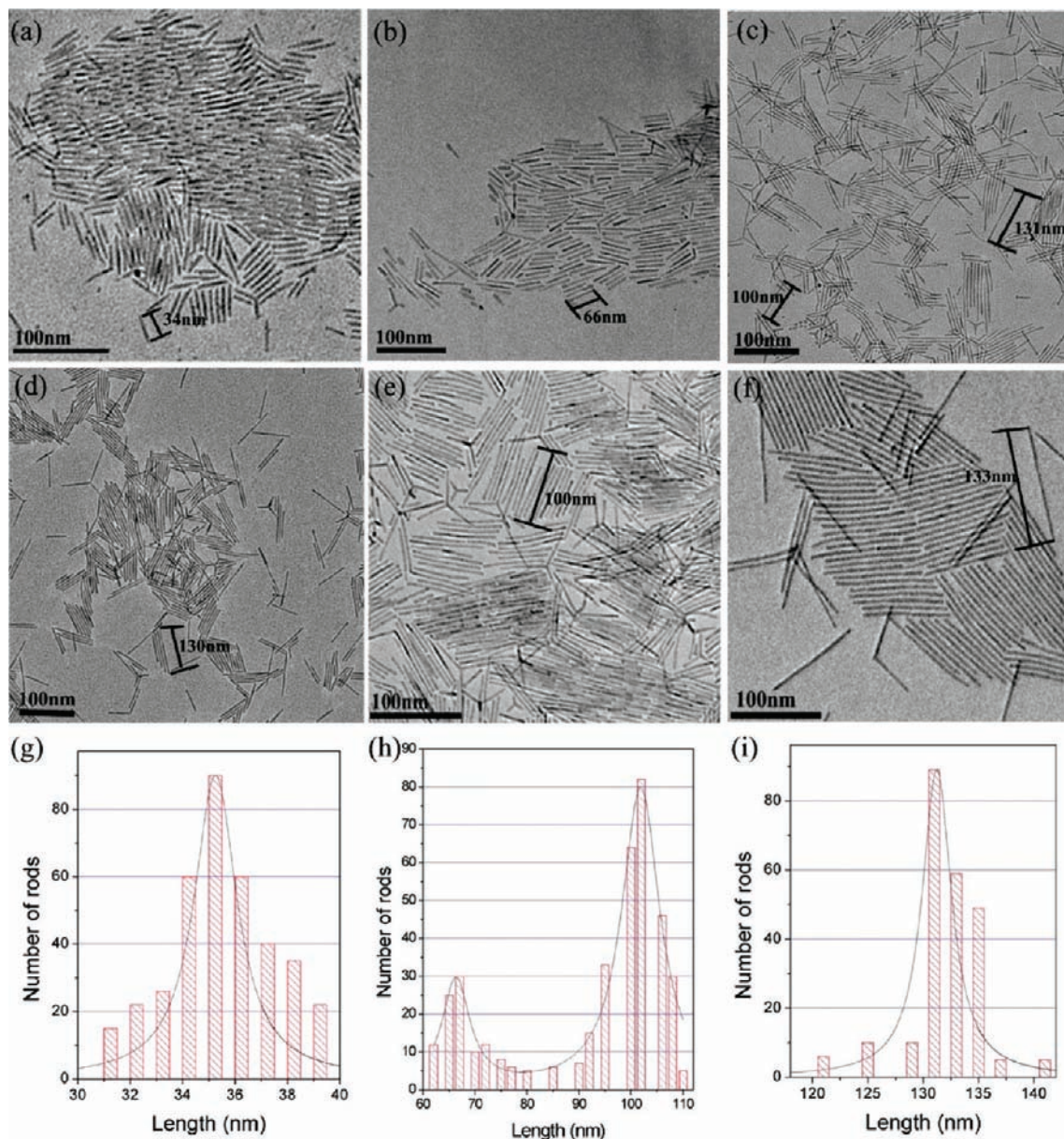
Figure 1. (a) TEM images of as synthesized CdS nanorods. (b) Elongated nanorods after a 30 s immersion in octylamine. (c) Elongated nanorods after a 120 s immersion in octylamine. (d) Elongated nanorods after a 30 s immersion in high concentration (0.030 mol) of octylamine. (e) Elongation after 30 s agitation in the presence of octylamine. (f) Elongation was observed after further addition of amine (0.018 mol) leading to monodispersed nanowires. Size distribution curves (g) correspond to the as synthesized nanorods showing the mean length of 34 nm, (h) corresponds to image *e* showing that the elongation is bimodial with some of the nanorods doubling and some tripling in length. (i) Size distribution curve of monodispersed nanorods imaged corresponding to image *f*.

joining area. Regardless of the extent of washing, further elongation was not observed beyond a factor of 4, suggesting a steric barrier to amalgamation when the aspect ratio limits end to end orientation in solution. Whereas the aspect ratio increased from 5 to 20, after the sequential washes the diameter of the nanorods at 7 nm remained unchanged. Some dipods, tripods and tetrapods that were present in the initial synthesis also elongated by oriented attachment of discrete rods on the end of each arm. The elongation process occurred instantaneously and for other amines that are liquid at room temperature such as decylamine, dipropylamine, hexylamine, diethylamine, dioctyl-amine tripropylamine, propylamine and trioctylamine, with slower reaction rates occurring for solid amines. A kinetic interpretation of the affect of temperature and concentration on elongation (see Supporting Information, S3–S7) shows an

activation energy of 14.3 $\pm$ 1.4 kJ/mol for the oriented attachment of the starting nanorods to their final length. This is a low activation energy compared to nanoparticle-nanoparticle attachment,[34,35] which explains the instantaneous nature of this reaction at room temperature.

High resolution (HR) TEM, was used to structurally char-acterize the elongated nanorods. A HRTEM image of two elongated nanorods is shown in Figure 2, where selected area FFT (fast Fourier transform) of 5 nm areas was used to determine the crystal direction. The main spots, corresponding to the (002) crystal plane, on the FFT inset in Figure 2a and b showed that there was a slight change in crystal direction when moving along the nanorod, visible by the slight angle change of the spots which is highlighted by the mirroring of the line from inset a to b. The measured interplanar spacing of the lattice
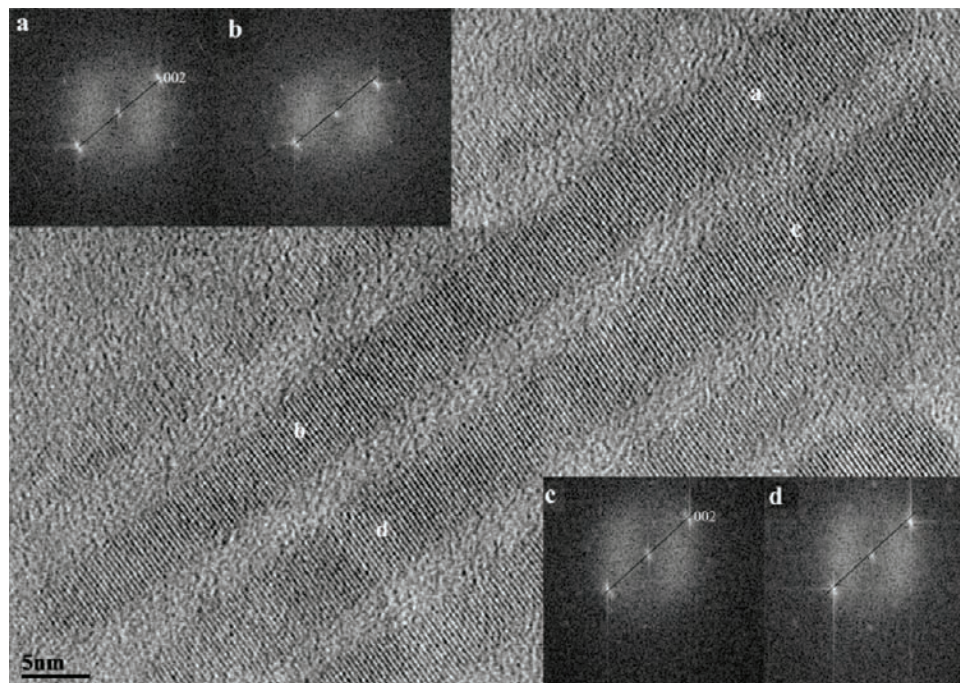
Figure 2. High resolution TEM montaged image of elongated nanorods, with selected area FFT insets. The letters in the FFT inset correspond to the area on the nanorod where the FFT measurement was taken from respectively and lines have been inserted and mirrored onto the adjoining image to further show the change in crystal direction.
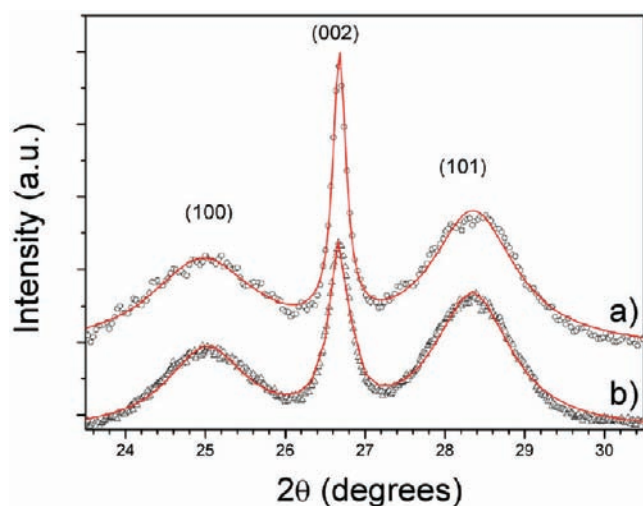

Figure 3. XRD spectra (a) nanorods subsequent to low concentration amine (0.018 mol) wash (b) as synthesized nanorods.

fringes on the (002) lattice plane was 0.33 nm, which corresponds to that of wurtzite CdS. The FFT patterns in Figure 2c and d show that there is also a change (1−2°) in crystal direction when traveling along the nanorod, which can either be attributed to rotation drift when imaging the area or due to two nanorods joining together.[30] The selected area FFT shows that the nanorods orient and attach along the same axis.

X-ray powder diffraction (XRD) measurements verified that the CdS nanorods were present in the wurtzite structure and remained unchanged after the oriented attachment, Figure 3 (see Supporting Information Figure S2 for full spectra). A noticeable feature of the diffractogram is the narrow (002) reflection, when compared with the other peaks in the spectra. Scherrer analysis of the peak broadening of all other peaks revealed crystallite dimensions of around 7 nm, while analysis of the (002) peak

returned a value of 31 nm, confirming the nanorod growth is along the *c*-axis and agreeing roughly with the dimensions observed from TEM imaging. The peaks for the (100), (002) and (101) reflections for both the amine washed and as-synthesized rods were fitted using a least-squares routine with pseudo-Voigt functions and the peak broadening measured. While there was no change in the broadening for the (100) and (101) reflections, there was a noticeable narrowing of peak width for the (002) reflection. Scherrer analysis showed that the crystallite dimension had increased from 31 to 52 nm, implying epitaxial attachment of the elongating rods. It is expected that the nanorods would double from this addition of amine, similar to Figure 1b. The shorter than expected double crystallite dimension can be accounted for by the presence of nonelongated rods and tetrapods in the XRD sample. Instrumental broadening was accounted for by measuring the broadening due to crystals of a crystallite size greater than 250 nm.

Polydispersity in nanorod diameter in the initial nanorods resulted in imperfect oriented attachment after a low concentration amine wash (0.018 mol). In Figure 4a, and further magnified in the inset, the fusion of two nanorods with diameters of 7 and 3 nm respectively is apparent after a single octylamine wash. Although, the diameters are significantly different, there is no evidence of a stacking fault along the (001) direction evident from the high resolution image. In figure 4b, similar fusion of nanorods of differing diameters is highlighted where in high resolution image inset a stacking fault is evident most likely due to infill growth occurring in the zinc blende crystal structure. The fault occurs over 2−3 atomic rows which is typical in anisotropic II−VI nanocrystals.[16]

To further investigate the mechanism of nanorod attachment, gold tips were grown symmetrically and asymmetrically onto the (001) facet of cadmium sulfide nanorods, with a starting nanorod length of ~45 nm. Initially a single gold tip was asymmetrically grown onto each nanorod, according to the route
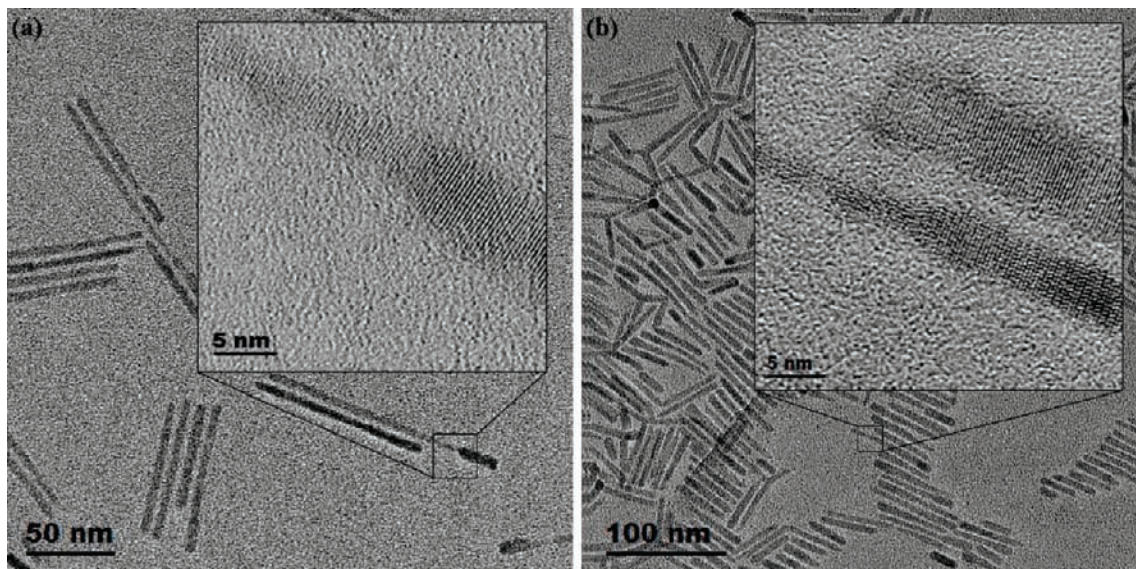
Figure 4. (a) TEM image of two different diameters nanorods attaching, with HRTEM insets magnifying the joining area. (b) TEM analysis of two nanorods with different diameters attaching leading to the occurrence of stacking fault.
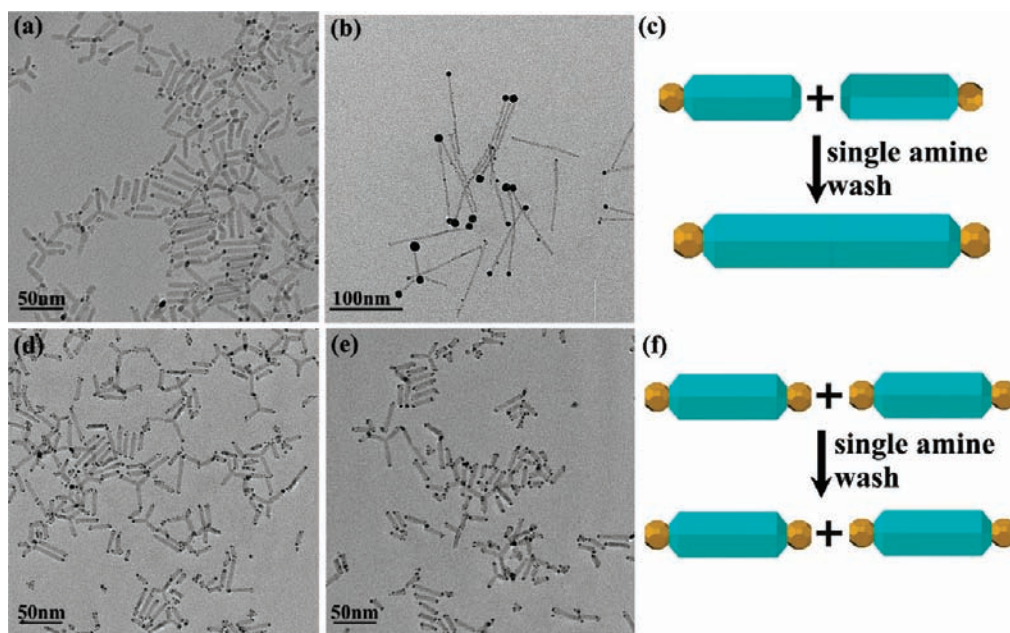

Figure 5. (a) CdS nanorods where gold is asymmetrically grown onto the (001) facets. (b) When subjected to octylamine it resulted in the attachment of these nanorods at the untipped side. (c) Schematic showing the attachment of the gold tipped nanorods due to a single octylamine wash. (d) CdS nanorods with symmetric gold growth onto the (001) facets. (e) When amine was added no attachment was seen. (f) Schematic showing the result of an amine wash on symmetric gold tipped nanorods resulting in no elongation due to the capping of the facets.

described by Banin,[37] as shown in Figure 5a. After a single octylamine wash these nanorods attach via the end facet of the nanorod diametrically opposite the gold tip resulting in a doubling of the starting nanorod length and the formation of symmetrically tipped nanorods (Figure 5b). Ripening of the gold also occurs during this process as can be seen by the resulting tips in Figure 5b where the tip size has almost doubled. When nanorods with gold tips symmetrically grown on the nanorods (Figure 5d) were subjected to an amine wash no elongation occurs regardless of amine concentration, Figure 5e. Clearly, the presence of gold nanoparticles on both ends of the nanorod

prevents end to end fusion. This lack of elongation on nanorods with symmetrically grown gold tips proves that oriented attachment of the nanorods is occurring in this elongation process. The uniform doubling of single gold tipped nanorods shows that solution phase attachment of nanorods is a dynamic process allowing nanorods to find their preferred orientation, at the untipped ends, before amalgamation.

Figure 6a and b shows UV−vis and PL analysis of the as synthesized and elongated CdS nanorods obtained after washing with different concentrations of octylamine. PL spectra of the same set of samples excited at a wavelength of 350 nm is shown in Figure 6a where the emission spectra were measured at room temperature with the nanorod sample dispersed in toluene. The

(37) Mokari, T.; Rotherberg, E.; Popov, I.; Costi, R.; Banin, U. *Science* **2004**, *304*, 1787–1790.
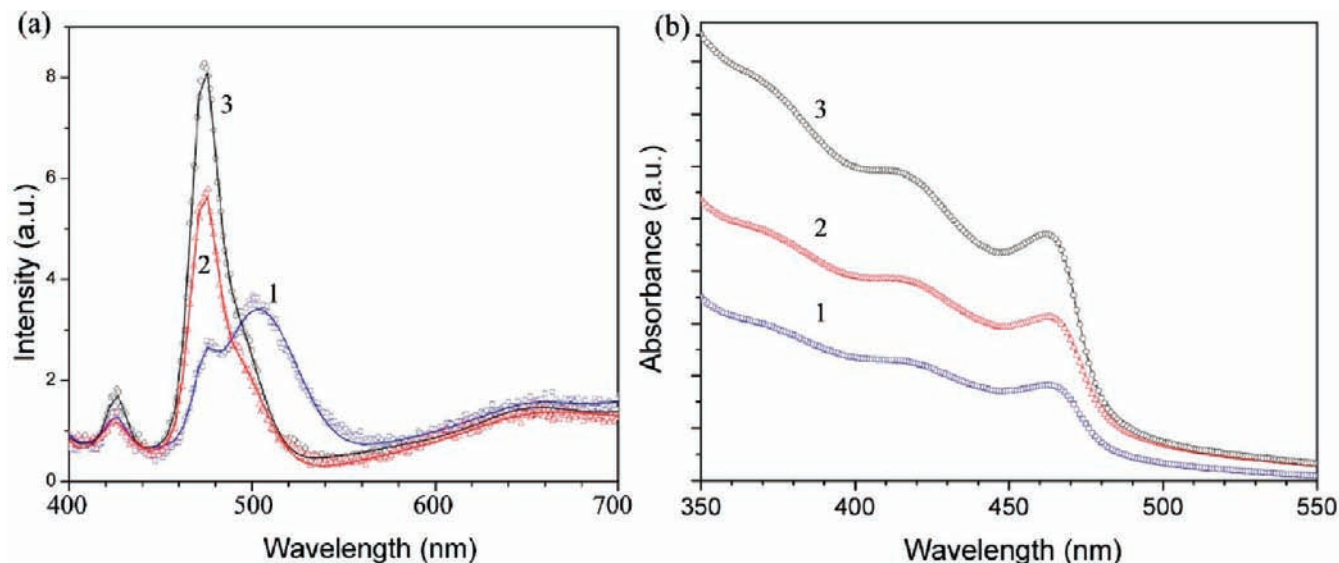
Figure 6. (a) Photoluminescence and (b) UV−vis measurements of the as-prepared CdS nanorods (curve 1), elongated nanorods after washing with low concentration (0.006 mol) octylamine (curve 2), and high concentration (0.024 mol) octylamine (curve 3).
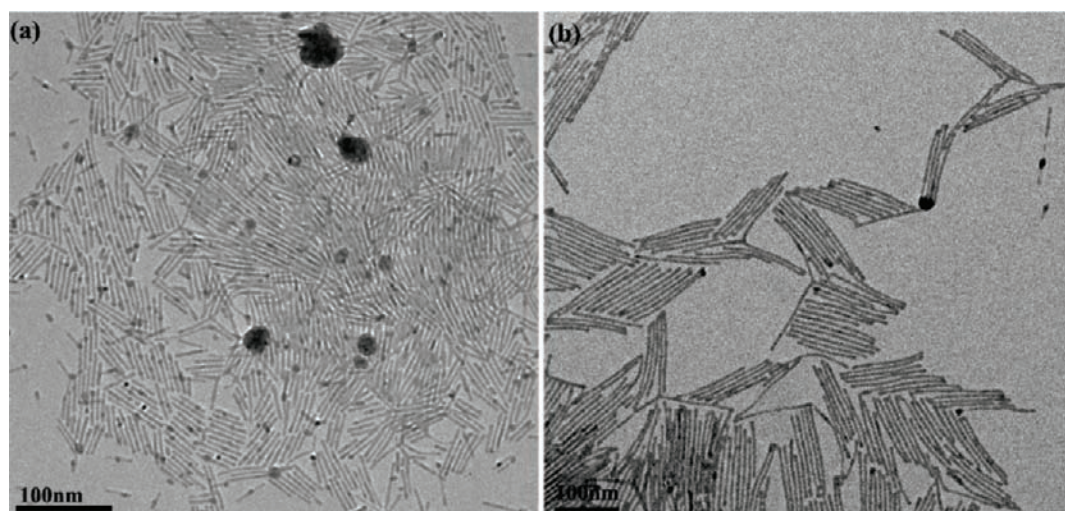

Figure 7. (a) Silver Sulfide (Ag2S) nanorods prepared by cation exchange from CdS. (b) Elongated Ag2S after a two amine washes with an average length of ∼120 nm.

PL spectra were fitted using a least-squares method. The spectra of the as synthesized nanorods (curve 1) exhibits two peaks: a narrow weak peak at ∼473 nm due to excitonic emission and a broad peak centered at ∼500 nm due to carrier recombination due to surface trap states of the CdS nanorod. After a low concentration (0.006 mol) octylamine wash (curve 2) PL analysis revealed that there is a significant intensity increase in excitonic enhancement at ∼473 nm and a reduction in surface trap states emission. The trap state emission relates to the surface chemistry and the structure of the nanorod. It has previously been reported that amines, which are electron donation molecules, decrease the amount of trap state emission.[5] Further increase in the amine concentration (0.024 mol) leads to an intense excitonic emission peak and a decrease in the amount of surface trap state emission (curve 3). This sharp, narrow emission peak for the CdS nanorods indicates monodispersity within the sample. The broad emission tail at wavelengths of ∼650 nm are commonly seen and can be accounted for due to deep level centers created by sulfur vacancies. The corresponding UV−vis absorbance spectra are shown in Figure 6b. The

as-synthesized CdS nanorods show an absorption peak centered at around 464 nm. This feature can be attributed to excitonic transitions in strongly quantized materials. There is no apparent difference in the position of the absorption maximum in the UV−vis spectra of the as-synthesized and nanorods subjected to amine.

Silver sulfide (Ag2S) nanorods were also subjected to an amine wash, where the starting nanorods were CdS and were fully cation exchanged to Ag2S (Figure 7a) as confirmed by XRD (see Supporting Information Figure S3). The silver precursor is AgNO3 and the concentration of AgNO3 relative to the concentration of the CdS nanorods determines the extent of cation exchange. At low concentrations partial cation exchange will take place, whereas at high concentrations the CdS nanorods will be fully exchanged.[38] The starting CdS nanorods were approximately 40 nm and remained dimensionally unchanged after the exchange to Ag2S nanorods. When

(38) Son, D. H.; Hughes, S. M.; Yin, Y.; Paul Alivisatos, A. *Science* **2004**, *306*, 1009–1012.

Table 1. XPS Analysis of CdS, CdSe and CdTe Samples As Synthesized (I) and after Octylamine Wash (II)

element	CdS (atomic %)		CdSe (atomic %)		CdTe (atomic %)	
	I	II	I	II	I	II
Cd 3d	33.9	41.1	34.5	34.5	34.5	48.3
X (S, Se, Te)	22.8	34.3	34.6	32.4	15.7	38.0
P 2p	43.3	24.5	30.9	33.1	49.8	13.7
Cd:P	0.78	1.68	0.99	1.04	0.70	3.64
Cd:X (S, Se, Te)	1.48	1.20	1.12	1.06	2.25	1.28

these Ag_2S nanorods were subjected to amine washes attachment occurred at the same rate as CdS nanorods of similar length. These Ag_2S nanorods contain the same easily destroyed ligands as CdS and so show similar attachment rates. After two octylamine washes these nanorods increased to a monodispersed length of 120 nm (Figure 7b) and the diameter of 7 nm remained unchanged throughout the washing steps. High resolution images show that the nanorods attach into "perfect oriented attached" nanowires, similar to those previously observed with attached CdS nanowires. The darker regions in both the starting and longer Ag_2S nanorods are commonly seen for fully cation exchanged Ag_2S.[38]

Equivalent amine washes on other II−VI nanorods; Cadmium Selenide (CdSe) and Cadmium Telluride (CdTe) showed differing results. No elongation occurred with CdSe nanorods in the presence of an amine regardless of concentration or reaction time (see Supporting Information Figure S4). In CdTe rods, the propensity for branched growth in the initial synthesis was enhanced during amine washing resulting in aggregated 3D network structures (see Supporting Information Figure S5) where it was difficult to determine the extent of elongation in a single crystallographic direction although attachment clearly occurs.

To fully understand the varying effects of the amine on the II−VI nanorods, the chemical compositions before and after a single octylamine wash were studied using XPS. High resolution photoelectron spectra of Cd 3d, S 2p, Se 3d, Te 3d and P 2p were measured and quantified to determine the relative atomic concentrations as shown in Table 3. P 2p appears at a binding energy of 133.1 eV and corresponds to P−O present in the ligands which are bound to the surface of the nanorods during synthesis. The Cd:P ratio increases significantly for both CdS and CdTe after the amine wash (Table 1) demonstrating partial removal of the ligands during the attachment of the nanorods. Cd 3d and P 2p photoelectron spectra clearly show this change for CdTe and CdS as synthesized and after an octyl amine wash (see Supporting Information Figure S6). The change in the Cd:P ratio is considerable for CdTe compared to CdS which is consistent with the enhanced degree of rod attachment seen for CdTe after the amine wash. The change in the Cd:P ratio for CdSe is insignificant and supports the observed absence of oriented attachment. While the extent of Cd−P ratio decrease in elongated CdS nanorods suggests ligand removal is not restricted only to the end facets, it is expected that the greater reactivity of the nanorod ends coupled with the greater thermodynamic stability of higher aspect ratio nanorods is the driving force for elongation. The mutual end to end attraction of the nanorods most likely occurs from dipole attraction due to the noncentrosymmetric wurtzite lattice with attachment along a common crystallographic orientation leading to the greatest reduction in surface energy. We can use the dipole−dipole potential formula

$$V(R_{12}, \theta_1, \theta_2, \phi) = -\frac{\mu_1\mu_2}{4\pi\varepsilon_0 R_{12}^3}(2\cos\theta_1\cos\theta_2 - \sin\theta_1\sin\theta_2\cos\phi) \quad (1)$$

to calculate the energy of the dipole attraction between the rods, where μ_i are the dipole moments; θ_i are the angles between the moments and the displacement vector (R_{12}); and φ is the torsion angle. For aligned identical rods, this simplifies to

$$V = -\frac{\mu^2}{2\pi\varepsilon_0 R_{12}^3} \quad (2)$$

where the interdipole displacement is given by the rod length. CdSe rods with dimensions of 30 × 5 nm measured by Li and Alivisatos have a dipole moment of 209.9 ± 32.6 D.[6] Since the dipole moment of CdS is 2.19 times that of CdSe, according to calculations by Nann and Schneider,[4] we can estimate that the dipole moment of CdS rods of identical dimensions would be 459.5 ± 71.4 D. Given that the dipole moment is observed to scale linearly with volume,[4,6] and taking into account that the use of different solvents will lead to a change in the effect of electric depolarisation, we calculate a value of $\mu = 601 \pm 93$ D for our CdS starting nanorods. The energy of the dipole attraction is then calculated to be 10.5 ± 3.2 meV. While this is comparable to the Boltzmann thermal energy at 25 °C (25.7 meV), it does not exceed it by orders of magnitudes as was observed for the dipole−dipole attraction of spherical nanoparticles.[30] Here the dipole−dipole attraction most likely only acts to orientate the nanorods in solution such that attachment can occur rather than providing the binding force for particle aggregation (see Supporting Information, S7−S8 for further details).

The reduction in the Cd:S ratio after a single amine wash is also interesting. Considering in a typical wash, as shown in figure 1d, 30% of the nanorods typically double with 70% tripling corresponding to a total surface area reduction of approximately 17%. This correlates closely with the reduction in the Cd:S ratio as calculated from XPS of 18%. This confirms, as expected, that the fusion of nanorods removes dangling bonds of Cd in the elongated with respect to the short nanorods. The greater decrease in Cd:Te ratio compared to Cd:S is also consistent with the greater number of attachment sites required for the formation of a branched 3d network as observed. The absence of ligand removal in CdSe after amine washing suggests a stronger binding of the ligand to the nanorods in this case confirming that selective ligand removal is the necessary requirement for nanorod growth. In the CdSe synthesis the coordinating ligand is tetradecylphosphonic acid (TDPA) whereas octadecylphosphonic acid (ODPA) was necessary for nanorod growth with CdS and CdTe suggesting a comparatively stronger binding of TDPA ligands to II−VI nanorods and the requirement of a stronger depassivating agent for oriented attachment to occur.

4. Conclusion

In summary we present an instantaneous approach that leads to the controllable end to end attachment of CdS and Ag_2S nanorods by manipulating the surface of the nanorods via an amine wash at room temperature. The acceleration of the oriented attachment is concentration and reaction time dependent and is thermodynamically driven due to the reduction of interfacial surface energy. The sequential nature of the attach-

ment results in highly monodisperse, single crystalline nanorods that are a controllable multiple of the original. Enhancement of electron transport properties is known to occur in single crystal nanowires as a function of length, hence these elongated nanorods are potentially applicable as electrically driven lasers.[39] The elongated II−VI nanorods may also create more efficient nanorod/polymer solar cells by providing more directed paths for charge transport and where tuning of the nanorod length to the device thickness can lead to optimal absorption of the incident light.[12,40]

Supporting Information Available: Further experimental details, reaction kinetics, dipole−dipole attraction, XRD of starting CdS nanorods, elongated nanorods and cation exchanged Ag₂S, TEM analysis of CdSe and CdTe nanorods prior to a subsequent to amine washes, XPS spectra of the as synthesized CdS and CdTe nanorods and subsequent to amine washing. This material is available free of charge via the Internet at http://pubs.acs.org.

JA902860T

(39) Duan, X.; Huang, Y.; Agarwal, R.; Lieber, C. M. *Nature* **2003**, *421*, 241–245.
(40) Kang, Y.; Kim, D. *Sol. Energy Mater. Sol. Cell* **2006**, *90*, 166–174.